European Spine Journal (2019) 28:3076–3084
https://doi.org/10.1007/s00586-019-06145-4

ORIGINAL ARTICLE

# Surgical outcome differences between the 3D subtypes of right thoracic adolescent idiopathic scoliosis

Saba Pasha[1,2] · Keith Baldwin[1]

Received: 29 May 2019 / Revised: 13 August 2019 / Accepted: 7 September 2019 / Published online: 24 September 2019


## Abstract

**Background** The current classifications of adolescent idiopathic scoliosis (AIS) aim to guide surgical decision making. However, variance exists within treatment recommendations and suboptimal outcomes have been observed while following these guidelines based on two-dimensional images. We used previously developed 3D classification for right thoracic AIS patients and aimed to determine the variation in surgical decision making and the risk of suboptimal outcomes in each subtype according to our classification.

**Methods** Seventy-six right thoracic AIS patients with 2-year follow-up were included retrospectively. Five 3D preoperative subgroups were determined based on a previous classification system. The upper and lower instrumented vertebrae (UIV and LIV) and the radiographic surgical outcomes at 2-year [frontal balance (FB), proximal junctional kyphosis (PJK), and adding on] were compared between the subtypes.

**Results** The fusion length and the rate of radiographic suboptimal outcomes were statistically different between the five groups. LIV at T12 in Type 1 and UIV at T2 in Type 2 were associated with improved FB and lower PJK, respectively. Type 3 had the highest rate of suboptimal FB and developing PJK. Type 4 had the longest fusion, and suboptimal FB was observed in 42% of the patients independent from the LIV level. Type 5 had the lowest rate of unsatisfactory radiographic outcomes at 2 years.

**Conclusion** Following the preoperative 3D classification of the AIS patients, we showed that the UIV and LIV selection has a different impact on the surgical outcomes in each of the five subtypes. The proposed 3D classification has the potential for risk stratification following a posterior spinal surgery in right thoracic AIS.

### Graphic abstract

These slides can be retrieved under Electronic Supplementary Material.

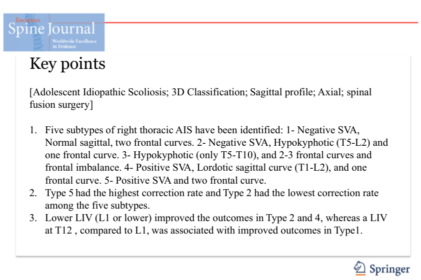


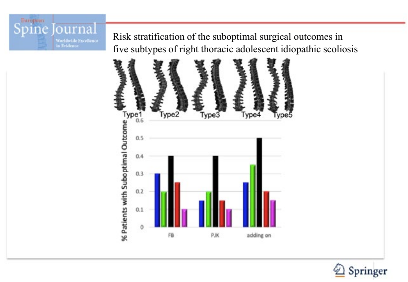


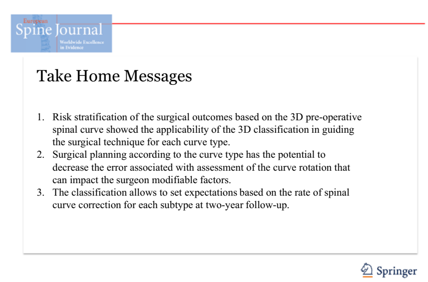


**Keywords** Adolescent idiopathic scoliosis · 3D classification · Sagittal profile · Transverse plane · Spinal fusion surgery

**Electronic supplementary material** The online version of this article (https://doi.org/10.1007/s00586-019-06145-4) contains supplementary material, which is available to authorized users.

✉ Saba Pasha
pashas@email.chop.edu

Extended author information available on the last page of the article

## Introduction

Posterior spinal fusion surgery remains the treatment of choice for severe, progressive spinal deformities in adolescent idiopathic scoliosis (AIS). The preoperative spinal curvature characteristics are important factor in surgical decision making [1]. As such, these characteristics in both two dimensions (2D) and three dimensions (3D) have been used in several classifications to guide surgery [2–5]. Limitations of 2D classifications in surgical decision making have been highlighted in past studies, which have suggested a need to consider additional criteria [6, 7].

Scoliosis is a 3D deformity, and as such, it stands to reason that consideration of the axial plane may carry at least as much prognostic significance as the coronal and sagittal planes. Tomograms and stereoradiography technology are putting 3D technology more in reach for orthopedic clinics. However, a classification that takes into account the 3D shape of the spine, without a need for complicated image postprocessing, has not been made readily available to average orthopedic clinics [3, 8].

We previously developed a 3D classification of the spinal curve in right thoracic AIS [9]. This 3D classification identified subtypes of patients using a 3D model of the spine; however, we have subsequently noted that the subgroups could be extrapolated from a pair of frontal and sagittal curve patterns, i.e., standard 2D images. In the current study, we aimed to determine the differences in the fusion levels and the surgical radiographic outcomes of these subtypes of right thoracic AIS patients. The differences in the surgical outcomes as they relate to the fusion levels in each subtype were discussed.

## Materials and methods

### Subjects

After ethical board approval, a total of 76 consecutive right thoracic AIS patients treated with posterior spinal fusion with 2-year follow-up were retrospectively reviewed. All patients had biplanar spinal radiographs at preoperative, within one-month postoperative (early postoperative), and 2-year follow-up. Patients with a prior spinal surgery, spondylolysis, spondylolisthesis, spinal deformity diagnosis other than idiopathic scoliosis and neuromuscular conditions were excluded. Preoperative bending films assessed the flexibility of the curves in the frontal plane. All patients had direct vertebral rotations with one rod in. Four surgeons performed the surgeries.

### Image processing and classifications

We used a 3D classification method to group the cohort at preoperative visit into five subtypes. The classification method is described in detail in our previous work [9]. Briefly, to develop the 3D classification, the normalized 3D line connecting the vertebral centroids and a hierarchical classification determined the maximum number of the subgroups with distinctive pairs of frontal and sagittal curves in a cohort of 103 patients [9]. A total of five subgroups were identified based on this analysis. Figure 1 shows the five subgroups in frontal, sagittal, and axial views. The global gravity axis was used to generate the axial view. The specifications of each subtype are as follows:

**Type 1**: Normal thoracolumbar kyphosis [2, 4]. C7 is posterior to sacrum, thus a negative sagittal vertical axis (SVA). In the posterior view, T1 is leveled or tilted to the right. The direction of vertebral rotation, determined by the pedicles position, changes in the thoracolumbar region (*S*-shaped axial view).

**Type 2:** In the sagittal view, negative SVA and hypokyphotic (stacked-up vertebrae) at both T5–T10 and T10–L2. In the posterior view, T1 is leveled or tilted to the left. The direction of vertebral rotation changes in the lower lumbar region (*V*-shaped axial view).

**Type 3:** Hypokyphotic (only T5–T10), negative or close to zero SVA, and frontal imbalance. In the posterior view, T1 is leveled or tilted to the right. The direction of the vertebral rotation changes in thoracolumbar region (*S*-shaped axial view).

**Type 4:** Flat or lordotic sagittal profile with positive SVA, high (above midpoint) sagittal inflection point, and slight frontal imbalance. T1 is leveled or tilted to the left in the posterior view. The vertebral rotation changes direction in the lower lumbar region (*V*-shaped axial view).

**Type 5:** Hypokyphotic and forward trunk shift (positive SVA) with a low inflection (below midpoint) point and a proximal kyphosis curve. T1 is leveled or tilted to the right (posterior view). The direction of vertebral rotation changes in thoracolumbar region (*S*-shaped axial view).

Radiographic parameters were calculated for each cluster at preoperative, early postoperative, and 2-year follow-up: main thoracic Cobb angle (MTC), main thoracic apical vertebra rotation (AVR) and translation (AVT), lumbar Cobb angle (LC), lumbar AVR and AVT, thoracic kyphosis (TK) between T1–T4 and T4–T12 levels, L1–S1 lumbar lordosis (LL), pelvic incidence (PI), frontal and sagittal balances, and neutral vertebra and end vertebra (NV and EV). These parameters were measured using the 3D model of the spine to avoid erroneous 2D measurements [10–12]. The radiographic parameters, flexibility, and the correction rates were compared between the subtypes using an ANOVA or Kruskal–Wallis when appropriate. The Lenke-type distributions, shoulder balance, and the LIV with respect to the NV were determined.

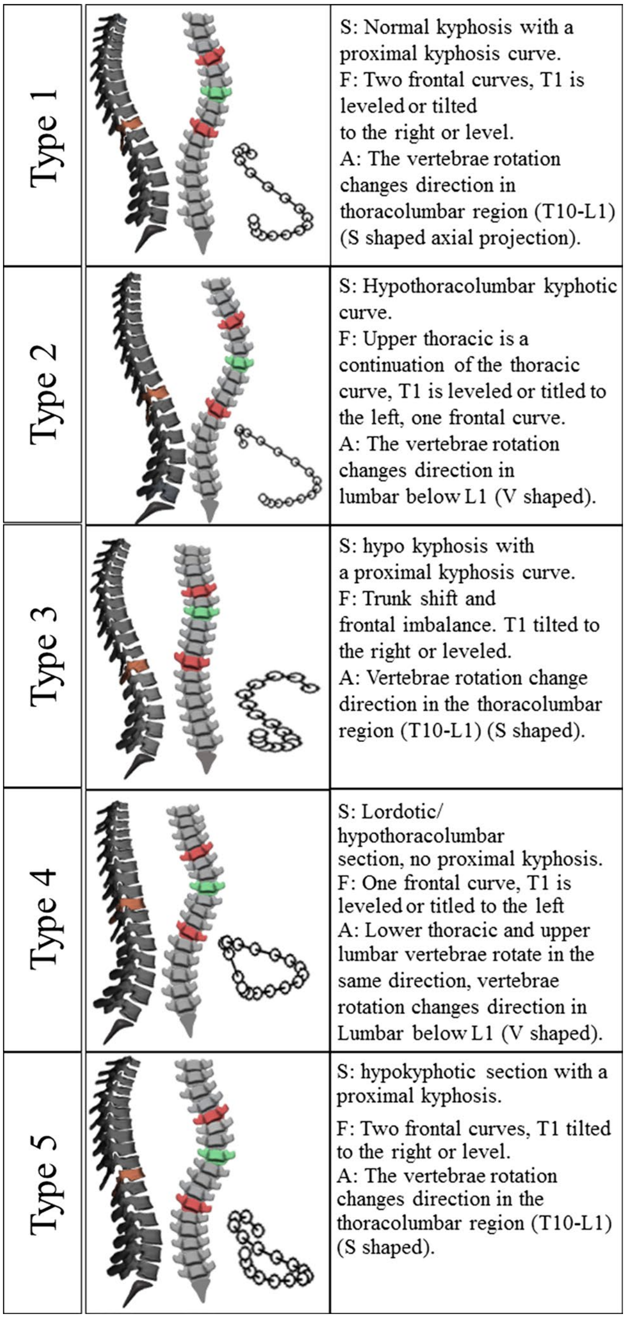


**Fig. 1** Five types of spinal alignment at preoperative. To determine the 3D subtype using the PA and lateral radiographs in *natural standing:* 1—determine the location of the changes in the vertebral axial rotation: if thoracolumbar Types 1, 3, or 5, if L2 or lower or the vertebrae did not change direction below the thoracic curve Types 2 or 4. 2—Determine SVA < 0 (Types 1, 2) or SVA ≥ 0 (Types 3, 4, 5). 3—Assign Type 3 (as opposed to 5), if there is a frontal trunk shift with three curves where thoracic and lumbar have similar magnitudes. The global gravity axis was used to generate the axial view

## Surgical assessment

The upper and lower fusion levels (LIV, UIV) were noted. UIV was selected based on shoulder balance: T2 left shoulder high, T3 for balanced shoulders, T4 right shoulder high [13]. The LIV was at neutral vertebra (NV) when NV and end vertebra (EV) were less than two levels apart and fused to NV-1 when this gap exceeded two levels.

The 2-year outcomes were evaluated in three categories: frontal balance, PJK, and adding on considering the following criteria. Ultimately, these three criteria were used to establish whether outcome was optimal or suboptimal.

## Frontal imbalance

C7 vertebrae shifted more than 1 cm away from the central sacral line in the frontal plane [14].

## PJK

At least 10° increase in the kyphosis angle was measured between the UIV and two supra-adjacent vertebrae between preoperative and 2-year follow-up [15, 16].

## Adding on

At least 5° increase in disk wedging below LIV or an increase in Cobb angle exceeding 5° [17, 18] was noted. The percentage of patients with suboptimal outcomes at 2 years were compared between the subgroups using a Chi-square test. Finally, the rates of suboptimal outcomes for different fusion levels in each subgroup were evaluated.

# Results

## Patient population

The average age at the time of preoperative radiographs was $14 \pm 3$. Eighty-three percent of the patients were female. The cohort was comprised of Type 1 ($n = 14$), Type 2 ($n = 17$), Type 3 ($n = 6$), Type 4 ($n = 21$), Type 5 ($n = 18$). Figure 2 shows the spinal curves for the five subtypes at three time points. Table 1 summarizes the distribution of the Lenke classification, shoulder height asymmetry, and the fusion level with respect to the neutral vertebra for the five subtypes. The distribution of kyphosis modifiers was significantly different between Types 1, 4, and 5, $p < 0.05$, and that of lumbar modifiers was significantly different between Types1 and 3, $p < 0.05$. The LIV with respect to NV was significantly different between Types 1, 3, and 5, $p < 0.05$.

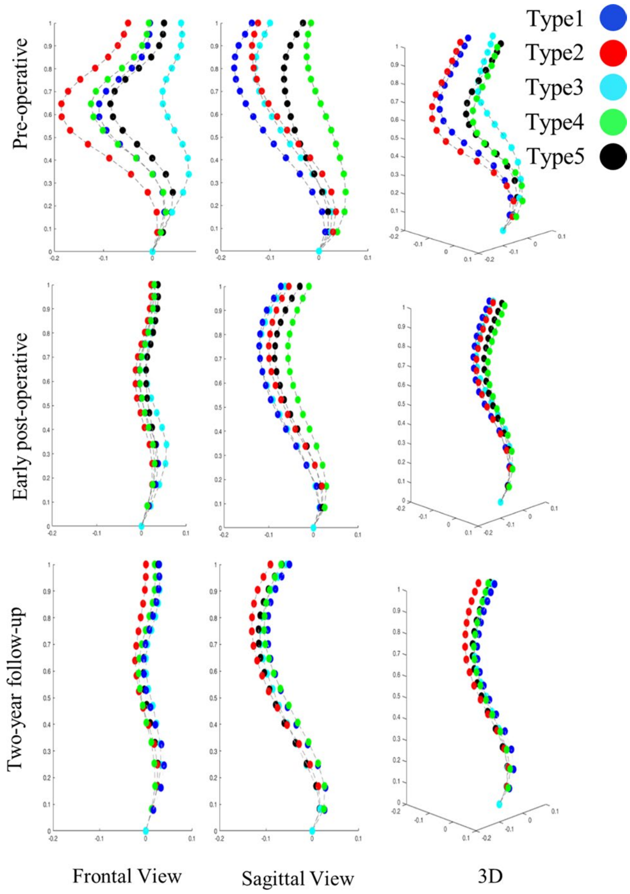


**Fig. 2** Frontal, sagittal, and 3D view of the spinal types at preoperative, early postoperative, and 2-year follow-up in the five subtypes of right thoracic scoliosis

## Curve flexibility

The rate of the thoracic curve flexibility was significantly different between the subtypes ($p = 0.03$); it was the highest in Type 5 (75% ± 23, 95% CI [66–83]) and the lowest in Type 2 (58% ± 11, 95%CI [45–64]). The rate of lumbar Cobb angle reducibility did not differ significantly between the five types, $p = 0.07$.

## Fusion lengths

The average number of fused vertebrae in the five subtypes was: Type 1, 9.6 ± 0.8, 95% CI [9.2–10]; Type 2, 10.3 ± 1.1, 95% CI [9.8–10.8]; Type 3, 8.5 ± 1.0, 95% CI [7.7–9.3]; Type 4, 10.0 ± 1.2, 95% CI [9.6–10.5]; and Type 5, 9.4 ± 1.1, 95% CI [8.9–9.9]. Type 3 had a significantly shorter fusion length compared to both Type 2 and Type 4, $p < 0.05$ (Fig. 3).

## Pre- and postoperative changes in spinal parameters in five subgroups:

Table 2 summarizes the radiographic parameters (mean and standard deviation) in the five types at preoperative, early postoperative, and 2-year follow-up. The preoperative lumbar Cobb angle, lumbar AVR, thoracic and lumbar AVT, TK (both T1–T4 and T4–T12), lumbar lordosis, and frontal and sagittal balances were significantly different between the five subtypes ($p < 0.01$). Table 2 also shows the results of the post hoc test between the five types for these parameters.

Between preoperative and early postoperative, there were significant differences in percent thoracic Cobb angle correction ($p = 0.03$) and percent lumbar Cobb angle correction ($p = 0.04$) between the five groups. Type 5 curves had the highest rate of percent thoracic Cobb angle correction (86.1% ± 11.8, 95% CI [80.3–91.1]), whereas Type 1 (64.2% ± 18.3, 95% CI [53.6–75]) and Type 2 (62.0% ± 15.2, 95% CI [55.9–70.1]) had the lowest percent correction. Type 4 had the highest percent lumbar curve correction (71.3% ± 17.7, 95% CI [63.0–79.6]), whereas Type 3 had the lowest percent rate lumbar correction (40.8% ± 20.3, 95% CI [20.7–60.9]).

At 2-year postoperative, there were significant differences between the subtypes in thoracic AVT ($p = 0.02$) and lumbar AVT ($p = 0.00$). The rate of thoracic AVT correction between the pre- and 2-year postoperative was the highest in Type 5 (141.0% ± 57.6, 95% CI [108.0–174.4]) and the lowest in Type 2 (100.5% ± 26.3, 95% CI [85.8–115.6]). The rate of lumbar AVT correction was the highest in Type

**Table 1** Lenke type distribution, shoulder asymmetry, and the LIV position with respect to the neutral vertebra for the five 3D subtypes

| | Lenke types % | | Lumbar modifiers % | | | Kyphosis modifiers % | | | Shoulder balance % | | | LIV with respect to neutral vertebra (NV) % | | |
|---|---|---|---|---|---|---|---|---|---|---|---|---|---|---|
| 3D subtypes | Lenke1 | Lenek2 | A | B | C | − | N | + | Right high | Level | Left high | NV-1 | NV | NV+1 |
| Type 1, $n = 14$ | 86 | 14 | 18 | 48 | 24 | 18 | 62 | 30 | 35 | 40 | 25 | 0 | 93 | 7 |
| Type 2, $n = 17$ | 92 | 8 | 25 | 39 | 36 | 23 | 58 | 18 | 0 | 70 | 30 | 47 | 47 | 6 |
| Type 3, $n = 6$ | 69 | 31 | 0 | 0 | 100 | 66 | 34 | 0 | 33 | 33 | 33 | 66 | 33 | 0 |
| Type 4, $n = 21$ | 100 | 0 | 0 | 33 | 66 | 89 | 11 | 0 | 44 | 47 | 8 | 43 | 56 | 0 |
| Type 5, $n = 18$ | 87 | 13 | 0 | 62 | 38 | 87 | 13 | 0 | 1 | 26 | 73 | 0 | 100 | 0 |

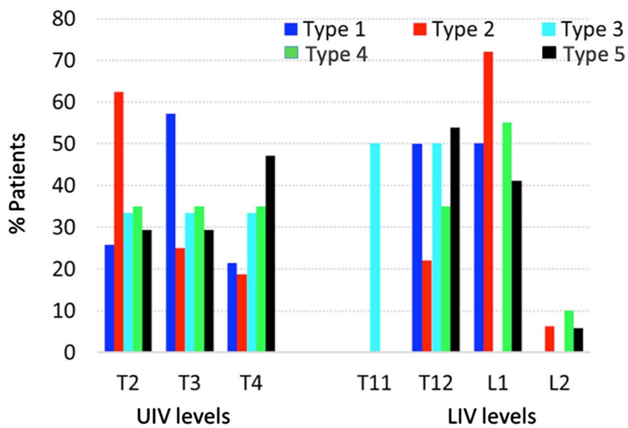


**Fig. 3** Position of upper and lower instrumented vertebrae (UIV and LIV) in the five subtypes

4 (119.0% ± 99.3, 95% CI [76.3–162.0]) and the lowest in Type 2 (21.6% ± 57.2, 95% CI [11.1–54.2].

## Surgical optimal/suboptimal outcome assessment:

The percent of suboptimal outcomes in each type is shown in Fig. 4 according to the definition of the optimal and suboptimal outcomes in Methods section. Type 3 had the highest and Type 5 had the lowest percent of suboptimal radiographic outcomes in the three categories of frontal balance, PJK, and adding on at 2 years.

In Type 1, six out of eight patients with a fusion to L1 had a frontal imbalance at 2 years, whereas only one out of seven patients with a fusion to T12 had a frontal imbalance. In Type 2, 51% of patients with a fusion to T2 developed a PJK; this percent decreased to 14% (one out of seven) for a UIV at T3 or T4. In Type 4, the rate of adding on for a LIV at T12 was 55% (five out of nine) and 1% for LIV at L1 (one out of ten).

## Discussion

We tested the utility of a 3D classification of right thoracic AIS patients as it relates to the 2-year outcomes of the posterior spinal fusion. Different rates of curve correction and percent of suboptimal outcomes in each of the five subtypes at 2-year follow-up suggested that considering the pair of frontal and sagittal spinal curves at preoperative, as suggested by our classification system (Fig. 1) [9], can differentiate between patient groups with different rates of curve correction or risk of suboptimal radiographic outcomes and set expectation for the surgeons and the patients.

Among the five groups, Type 5 had the lowest rate of suboptimal surgical radiographic outcomes, whereas Type

**Table 2** Clinical parameters of the five subtypes before surgery, at early postoperative (within a month), and at 2-year follow-up

| | Type | Thoracic Cobb (°) | Lumbar Cobb (°) | TAVR (°) | LAVR (°) | TAVT (°) | LAVT (°) | TK1-4 (°) | TK4-12 (°) | LL L1-S1 (°) | PI (°) | SS (°) | FB (mm) | SB (mm) |
|---|---|---|---|---|---|---|---|---|---|---|---|---|---|---|
| Preoperative | 1 | 60.0 ± 7.0 | 39.0 ± 6.5 | −12.6 ± 5.4 | 14.3 ± 2.4$^{\S}$ | −42.5 ± 7.1$^{\sim}$ | 13.6 ± 4.7 | 13.5 ± 9.1$^{\S}$ | 22.3 ± 9.6$^{\S}$ | 52.8 ± 11.4 | 47.0 ± 13.6 | 44.2 ± 11.8 | −0.2 ± 14.5 | −26.3 ± 18.3$^{\S,**}$ |
| | 2 | 65.8 ± 11.9 | 44.7 ± 11.1$^{\S}$ | −13.8 ± 8.2 | 10.4 ± 4.7 | −63.2 ± 14.8$^{\sim}$ | 2.5 ± 7.0$^{\sim}$ | 8.7 ± 6.5 | 17.1 ± 11.3 | 59.7 ± 8.4$^{\S}$ | 52.8 ± 14.0 | 43.2 ± 15.3 | −6.7 ± 9.5$^{\sim}$ | −23.3 ± 21.3$^{\S,**}$ |
| | 3 | 57.8 ± 8.2 | 42.4 ± 9.1 | −7.7 ± 8.9 | 6.4 ± 9.2 | 9.5 ± 19.4 | 18.0 ± 15.0$^{\dagger}$ | 15.6 ± 10.6$^{\S}$ | 20.8 ± 12.1$^{\S}$ | 51.2 ± 6.4 | 43.5 ± 13.2 | 39.6 ± 11.4 | 8.6 ± 10.6$^{\dagger}$ | −20.1 ± 21.0$^{\S,**}$ |
| | 4 | 57.7 ± 10.0 | 40.4 ± 8.0 | −9.5 ± 7.0 | 8.8 ± 5.6 | −40.9 ± 10.9$^{\sim}$ | 13.0 ± 5.3 | 18.4 ± 11.6 | 8.9 ± 7.1 | 52.3 ± 9.6 | 56.3 ± 7.6 | 47.6 ± 10.3 | −4.0 ± 15.2 | 0.4 ± 15.8 |
| | 5 | 56.1 ± 11.9 | 35.5 ± 2.3$^{\dagger}$ | −6.0 ± 6.1 | 5.0 ± 4.8$^{*}$ | −28.0 ± 14.3 | 15.4 ± 7.1 | 5.8 ± 6.5$^{\sim}$ | 7.8 ± 3.7$^{\sim}$ | 46.4 ± 5.3$^{\dagger}$ | 48.8 ± 10.2 | 40.4 ± 9.8 | 13.4 ± 4.7 | 5.2 ± 12.7 |
| Early post-operative | 1 | 21.5 ± 10.3 | 18.9 ± 10.4 | 6.4 ± 6.3 | 9.2 ± 4.2 | −2.7 ± 9.1 | 14.0 ± 7.3 | 11.0 ± 5.8 | 25.8 ± 7.3 | 51.4 ± 14.4 | 46.8 ± 14.2 | 41.0 ± 9.8 | 7.4 ± 8.4 | −2.1 ± 25.5 |
| | 2 | 24.4 ± 16.4$^{**}$ | 26.5 ± 14.7$^{\S}$ | 2.8 ± 6.5 | 6.7 ± 6.5 | −8.2 ± 9.5 | 9.4 ± 8.9 | 9.7 ± 4.6 | 22.3 ± 9.8 | 56.2 ± 12.3 | 51.1 ± 15.8 | 42.3 ± 10.8 | 6.7 ± 8.3 | −25.9 ± 19.2 |
| | 3 | 17.6 ± 13.8 | 25.1 ± 12.4 | 4.3 ± 5.0 | 4.6 ± 5.7 | 15.5 ± 13.5 | 19.1 ± 14.6 | 14.2 ± 6.7 | 21.7 ± 5.1 | 49.5 ± 10.6 | 46.7 ± 15.2 | 36.9 ± 9.3 | 10.5 ± 12.5 | −10.1 ± 10.4 |
| | 4 | 14.0 ± 10.1 | 10.1 ± 9.6† | 1.3 ± 8.0 | 2.7 ± 4.5 | −1.5 ± 12.6 | 11.4 ± 8.1 | 11.2 ± 6.9 | 18.3 ± 6.1 | 50.7 ± 6.7 | 55.0 ± 9.3 | 43.5 ± 5.7 | 7.6 ± 11.1 | −4.2 ± 16.8 |
| | 5 | 8.0 ± 9.6$^{\dagger}$ | 16.8 ± 11.6 | 3.5 ± 2.4 | 7.8 ± 5.0 | 14.0 ± 9.1 | 12.9 ± 11.6 | 8.2 ± 7.5 | 21.4 ± 4.8 | 46.6 ± 7.3 | 50.0 ± 11.2 | 37.7 ± 5.6 | 13.7 ± 11.1 | −11.5 ± 19.9 |
| Two-year follow-up | 1 | 20.7 ± 11.1 | 19.6 ± 9.7 | 0.5 ± 13.2 | 7.2 ± 5.3 | 8.8 ± 5.9 | 18.7 ± 4.7$^{\S}$ | 12.3 ± 6.2 | 28.5 ± 4.7 | 65.6 ± 13.0 | 48.4 ± 13.3 | 46.2 ± 9.2 | 11.2 ± 4.9 | −8.0 ± 26.5 |
| | 2 | 26.5 ± 18.4$^{**}$ | 22.2 ± 13.2 | 2.2 ± 10.1 | 9.1 ± 6.9 | −0.4 ± 11.5$^{**}$ | 12.1 ± 11.9 | 8.9 ± 5.9 | 26.3 ± 8.9 | 55.6 ± 11.2 | 50.8 ± 13.6 | 38.6 ± 12.3 | −0.9 ± 14.5 | −22.4 ± 19.2 |
| | 3 | 20.3 ± 15.6 | 17.2 ± 10.9 | −2.8 ± 4.9 | 5.4 ± 3.7 | 7.7 ± 14.2 | 9.2 ± 11.0 | 13.8 ± 8.1 | 23.1 ± 5.1 | 55.2 ± 7.1 | 42.3 ± 11.3 | 39.6 ± 6.6 | 10.9 ± 17.4 | −11.9 ± 22.4 |
| | 4 | 19.4 ± 9.0 | 12.6 ± 11.2 | 5.4 ± 7.8 | 9.2 ± 7.0 | −5.2 ± 15.8 | 1.9 ± 11.4$^{*}$ | 10.5 ± 7.9 | 22.8 ± 6.7 | 57.4 ± 8.1 | 54.7 ± 10.3 | 44.6 ± 6.5 | 5.9 ± 12.8 | −16.1 ± 23.3 |
| | 5 | 11.2 ± 11.4$^{\dagger}$ | 17.6 ± 9.6 | 4.0 ± 4.2 | 13.5 ± 7.3 | 11.2 ± 16.1$^{\dagger}$ | 8.5 ± 12.3 | 11.9 ± 4.9 | 20.5 ± 5.2 | 52.6 ± 7.4 | 48.0 ± 15.6 | 39.9 ± 7.4 | 8.0 ± 11.1 | −16.8 ± 9.0 |

Significantly different from $^{*}$Type 1, $^{\dagger}$Type 2, $^{\sim}$Type 3, $^{\S}$Type 4, $^{**}$Type 5, $p < 0.05$

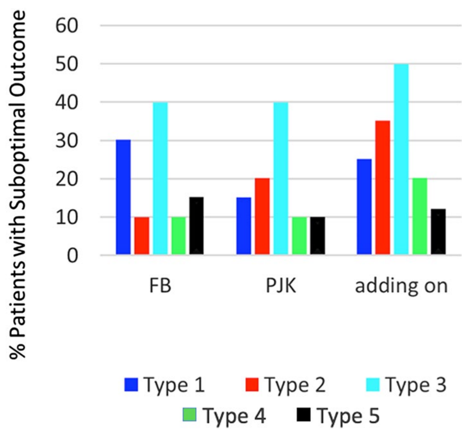


**Fig. 4** Percent number of patients with suboptimal outcomes in three categories (frontal balance, proximal junction kyphosis (PJK), and adding on) in five subtypes of right thoracic scoliosis

3 had the highest rate of suboptimal outcomes and on average the shortest fusion length among the five subtypes in our cohort. The LIV with respect to NV changed significantly between the groups. LIV was selected almost equally at NV-1 and NV in patient types with one curve (Types 2, 4) (Table 1). Small vertebral rotation in the thoracolumbar region (Fig. 1) may have resulted in NV misidentification [12]. The outcomes were improved as the LIV was at NV for these patients (Fig. 4). However, in the groups with two curves (Types 1, 3, and 5) due to the rapid change in the direction of the vertebral rotation between the two curves, EV and NV are closer and a fusion to NV-1 is recommended. This was also confirmed by our results that patients in these groups had better outcomes when LIV was at a higher level. Considering the proposed classification allows using the characteristics of the 3D curve patterns to better identify one versus two curves and decide for the LIV accordingly to avoid the error associated with LIV selection due to patient rotation and 3D curve deformity.

Different rates of suboptimal outcomes were observed between the subtypes (Fig. 4) which can assist with setting expectation for the outcomes or more rigorous subtype-specific surgical planning. The analysis of the suboptimal outcomes showed that Type 3 followed by Types 2 and 1 has the highest rate of unsatisfactory outcomes (Fig. 4). Type 3 had a preoperative frontal imbalance, and in our series, these patients had the shortest fusion lengths (Fig. 3). As we did not have any patient with a lower LIV level (lumbar spine) in this subtype, we could not verify whether a different fusion length could improve the surgical outcomes. In Type 2, more than 50% of the patients with a fusion to T2 developed a PJK while this risk deceased to 14% when a lower UIV (T3-T4) was selected. As the proximal thoracic is part of the main thoracic curve in these patients (Fig. 1), a lower UIV may have allowed a spontaneous correction of the unfused proximal curve. In contrast to Types 2 and 3, Type 1 patients were balanced in the frontal plane and had a normal sagittal profile preoperatively [9, 19], and yet a high rate of suboptimal outcomes was observed in this group. Our results showed large changes in the sagittal profile of these patients between the pre- and early postoperative, particularly in the thoracic region (Table 2, Fig. 2). Such large changes may potentially have an adverse impact on the harmonious thoracic/lumbar alignment, disrupted the posterior ligaments, and resulted in suboptimal outcomes [20–22]. This finding underlines that an understanding of the sagittal profile deviation from the normative value is essential to avoid imparting large or unnecessary modifications in the sagittal plane. In Type 4, with a lordotic T5–L2 curve and a high sagittal inflection point, fusion can be extended to the lumbar spine to assure imparting *both* kyphosis and lordosis and a smooth transition between the fused and unfused spines. As an example, two Type 4 patients with different UIV and LIV are shown in Fig. 5. While preoperatively both patients have similar spinal curves in frontal and sagittal views, a LIV at L1 in patient B allows imparting and stabilizing the curve in the thoracolumbar region, resulting in improved sagittal profile and subsequently increased lumbar curve correction for this patient as compared to patient A. However, as both patients have acceptable frontal and sagittal balances at the follow-up, the goal of the surgery, i.e., smaller compensatory curve or saving motion segments, should be also considered to evaluate the outcomes. Finally, in Type 5, the high thoracic curve flexibility on the bending film can relate to the high correction rate and the lowest rate of suboptimal outcomes in this group. Future studies that relate the 3D shape of the spine to the spinal flexibility are warranted.

Despite the emphasis on the axial rotation of the spine in AIS [4, 9], rotational parameters are not currently implemented in the AIS classification. The top-down view of the spine in the five clusters showed two different patterns: a *S-shaped* curve in Types 1, 3, and 5 and a *V-shaped* curve in Types 2 and 4 (Fig. 1) [9]. These axial views show intrinsic differences in thoracic and lumbar orientation between the clusters; In the *V-shaped* clusters, the vertebrae rotation in the lower curve changes direction in the lower lumbar area, whereas in the *S-shaped* groups, the lower curve starts rotating to the opposite direction in the thoracolumbar region (Fig. 1). In other words, in the axial view, the *S-shaped* groups have two distinct *curves*: one thoracic and one lumbar, whereas in the *V-shaped* types, the upper lumbar curve is an extension of the thoracic curve (Fig. 1). In the *V-shaped* group, a stack of vertebrae with no or nonsignificant rotation connect the thoracic curve to the lumbar vertebrae that only start rotating to the opposite direction in lower lumbar region indicating the start of a new 3D curve. This finding has implications for manipulating these two curve types (*S* and *V* shapes),

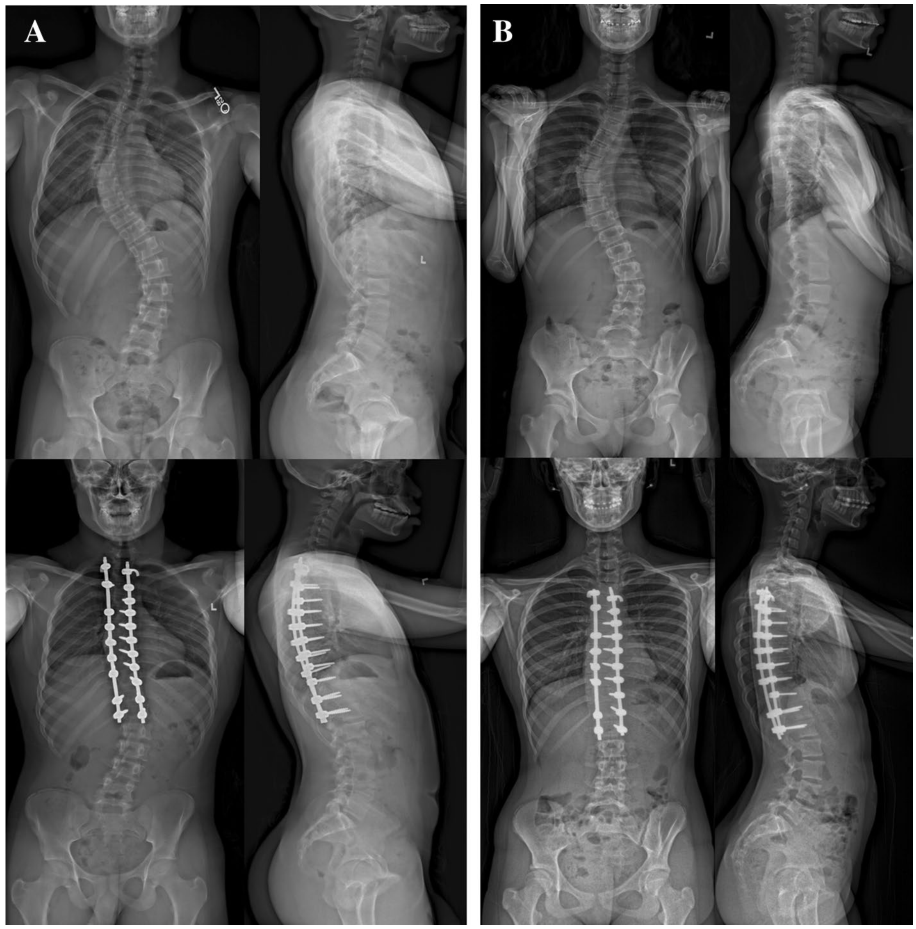


**Fig. 5** Examples of subtype 4 patients with different fusion levels and outcomes. A lower level LIV and higher lumbar Cobb correction were observed in patient B compared to patient A

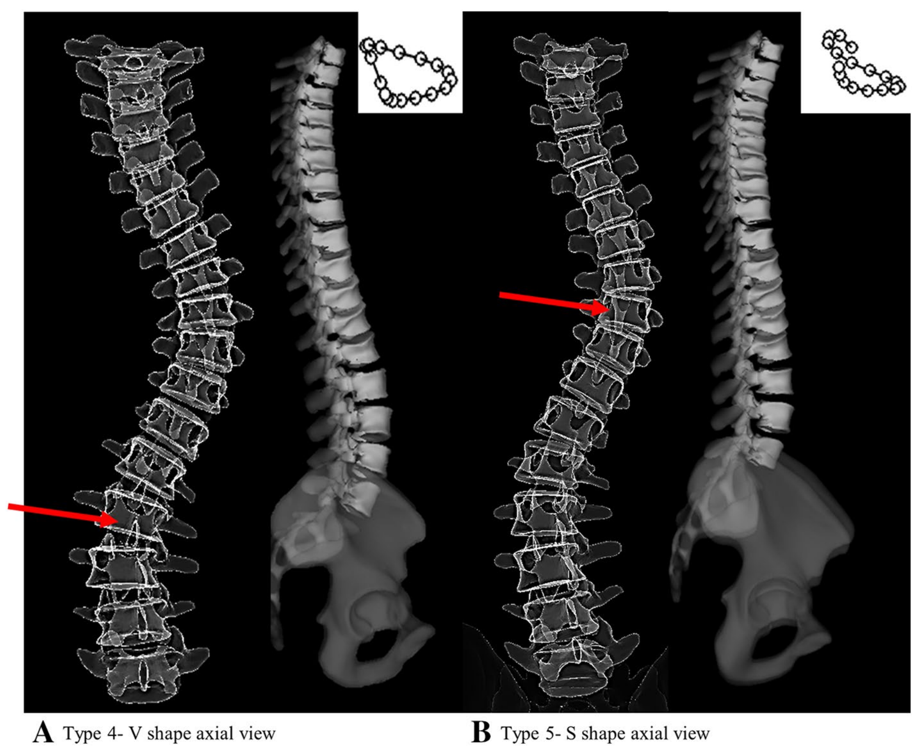


**Fig. 6** Changes in the direction of the vertebral rotation in patients with S-shaped and V-shaped axial curve patterns. In the *V-shaped* group, the direction of the vertebral rotation starts changing in the lumbar spine (Example A) whereas in the *S-shaped* groups, changes in the direction of the vertebral rotation occur in the thoracolumbar region (Example B). The global gravity axis was used to generate the axial view

either by selective versus nonselective fusion or by derotating and translation of different segments according to the curve type. An example of two patients with *V-shaped* (Type 4) and *S-shaped* (Type 5) axial curves is shown in Fig. 6. Despite the similar frontal curves between the two patients, in patient A the direction of vertebral rotation starts changing at L2 level and in patient B the direction of the vertebral rotation starts changing at T11 indicating a torsion in spine and the start of a new curve. Our classification draws attention to the differences in the frontal and sagittal curves as they relate to subtle difference in these 3D characteristics.

The new 3D classification of the right thoracic AIS identified subgroups of patients with distinguished characteristics in the frontal and sagittal planes. This classification allowed determining the risk of suboptimal outcomes associated with certain fusion levels in each group and can set expectation in each subtype. As the AIS surgery remains in part subjective, further validation in larger cohort and considering the biomechanics [23] and local changes in the disks within each subtype [24] allow application of this 3D classification in surgical planning and outcome prediction in AIS patients.

## Compliance with ethical standards

**Conflict of interest** The authors declare that they have no conflict of interest to disclose.

## References


1. Pasha S, Flynn J (2018) Data-driven classification of the 3D spinal curve in adolescent idiopathic scoliosis with an applications in surgical outcome prediction. Sci Rep 8:16296. https://doi.org/10.1038/s41598-018-34261-6
2. Lenke LG, Betz RR, Harms J, Bridwell KH, Clements DH, Lowe TG, Blanke K (2001) Adolescent idiopathic scoliosis: a new classification to determine extent of spinal arthrodesis. J Bone Joint Surg Am 83-A:1169–1181
3. Kadoury S, Labelle H (2012) Classification of three-dimensional thoracic deformities in adolescent idiopathic scoliosis from a multivariate analysis. Eur Spine J 21:40–49. https://doi.org/10.1007/s00586-011-2004-2
4. Abelin-Genevois K, Sassi D, Verdun S, Roussouly P (2018) Sagittal classification in adolescent idiopathic scoliosis: original description and therapeutic implications. Eur Spine J. https://doi.org/10.1007/s00586-018-5613-1
5. King HA, Moe JH, Bradford DS, Winter RB (1983) The selection of fusion levels in thoracic idiopathic scoliosis. J Bone Joint Surg Am 65:1302–1313
6. Chang KW, Leng X, Zhao W, Chen YY, Chen TC, Chang KI (2011) Broader curve criteria for selective thoracic fusion. Spine (Phila Pa 1976) 36:1658 1664. https://doi.org/10.1097/BRS.0b013e318215fa73
7. Pasha S, Flynn JM, Sankar WN (2018) Outcomes of selective thoracic fusion for Lenke 1 adolescent idiopathic scoliosis: predictors of success from the sagittal plane. Eur Spine J. https://doi.org/10.1007/s00586-018-5553-9
8. Stokes IA, Sangole AP, Aubin CE (2009) Classification of scoliosis deformity three-dimensional spinal shape by cluster analysis. Spine (Phila Pa 1976) 34:584–590. https://doi.org/10.1097/BRS.0b013e318190b914
9. Pasha S, Hassanzadeh P, Ecker M, Ho V (2019) A hierarchical classification of adolescent idiopathic scoliosis: Identifying the distinguishing features in 3D spinal deformities. PLoS ONE 14:e0213406. https://doi.org/10.1371/journal.pone.0213406
10. Pasha S, Cahill PJ, Dormans JP, Flynn JM (2016) Characterizing the differences between the 2D and 3D measurements of spine in adolescent idiopathic scoliosis. Eur Spine J 25:3137–3145. https://doi.org/10.1007/s00586-016-4582-5
11. Pasha S, Ecker M, Deeney V (2018) Considerations in sagittal evaluation of the scoliotic spine. Eur J Orthop Surg Traumatol 28:1039–1045. https://doi.org/10.1007/s00590-018-2175-1
12. DeFrancesco CJ, Pasha S, Miller DJ, Betz RR, Clements DH, Fletcher ND, Glotzbecker MG, Hwang SW, Kelly MP, Lehman RA, Lonner BS, Newton PO, Roye BD, Sponseller PD, Upasani VV, Harms Study G, Cahill PJ (2018) Agreement between manual and computerized designation of neutral vertebra in idiopathic scoliosis. Spine Deform 6:644–650. https://doi.org/10.1016/j.jspd.2018.03.001
13. Rose PS, Lenke LG (2007) Classification of operative adolescent idiopathic scoliosis: treatment guidelines. Orthop Clin North Am 38(521–529):vi. https://doi.org/10.1016/j.ocl.2007.06.001
14. Pasha S, Baldwin K (2018) Are we simplifying balance evaluation in adolescent idiopathic scoliosis? Clin Biomech (Bristol, Avon) 51:91–98. https://doi.org/10.1016/j.clinbiomech.2017.11.011
15. Kim YJ, Lenke LG, Bridwell KH, Kim J, Cho SK, Cheh G, Yoon J (2007) Proximal junctional kyphosis in adolescent idiopathic scoliosis after 3 different types of posterior segmental spinal instrumentation and fusions: incidence and risk factor analysis of 410 cases. Spine (Phila Pa 1976) 32:2731–2738. https://doi.org/10.1097/BRS.0b013e31815a7ead
16. Helgeson MD, Shah SA, Newton PO, Clements DH 3rd, Betz RR, Marks MC, Bastrom T, Harms Study G (2010) Evaluation of proximal junctional kyphosis in adolescent idiopathic scoliosis following pedicle screw, hook, or hybrid instrumentation. Spine (Phila Pa 1976) 35:177–181. https://doi.org/10.1097/BRS.0b013e3181c77f8c
17. Wang Y, Hansen ES, Hoy K, Wu C, Bunger CE (2011) Distal adding-on phenomenon in Lenke 1A scoliosis: risk factor identification and treatment strategy comparison. Spine (Phila Pa 1976) 36:1113–1122. https://doi.org/10.1097/BRS.0b013e3181f51e95
18. Lakhal W, Loret JE, de Bodman C, Fournier J, Bergerault F, de Courtivron B, Bonnard C (2014) The progression of lumbar curves in adolescent Lenke 1 scoliosis and the distal adding-on phenomenon. Orthop Traumatol Surg Res 100:S249–254. https://doi.org/10.1016/j.otsr.2014.03.012
19. Pasha S, Baldwin K (2019) Preoperative sagittal spinal profile of adolescent idiopathic scoliosis lenke types and non-scoliotic adolescents: a systematic review and meta-analysis. Spine (Phila Pa 1976) 44:134–142. https://doi.org/10.1097/BRS.0000000000002748
20. Cammarata M, Aubin CE, Wang X, Mac-Thiong JM (2014) Biomechanical risk factors for proximal junctional kyphosis: a detailed numerical analysis of surgical instrumentation variables. Spine (Phila Pa 1976) 39:E500–E507. https://doi.org/10.1097/BRS.0000000000000222
21. Ilharreborde B (2018) Sagittal balance and idiopathic scoliosis: does final sagittal alignment influence outcomes, degeneration rate or failure rate? Eur Spine J 27:48–58. https://doi.org/10.1007/s00586-018-5472-9

22. Pasha S, Ilharreborde B, Baldwin K (2019) Sagittal spinopelvic alignment after posterior spinal fusion in adolescent idiopathic scoliosis: a systematic review and meta-analysis. Spine (Phila Pa 1976) 44:41–52. https://doi.org/10.1097/BRS.0000000000002736
23. Pasha S, Aubin CE, Labelle H, Parent S, Mac-Thiong JM (2015) The biomechanical effects of spinal fusion on the sacral loading in adolescent idiopathic scoliosis. Clin Biomech (Bristol, Avon) 30:981–987. https://doi.org/10.1016/j.clinbiomech.2015.06.019
24. Pasha S, Smith L, Sankar WN (2019) Bone remodeling and disc morphology in the distal unfused spine after spinal fusion in adolescent idiopathic scoliosis. Spine Deform 7(5):746–753



## Affiliations

**Saba Pasha**[1,2] · **Keith Baldwin**[1]

[1] Division of Orthopedic Surgery, The Children's Hospital of Philadelphia, Philadelphia, PA, USA

[2] Department of Orthopedic Surgery, University of Pennsylvania, Perelman School of Medicine, Philadelphia, PA, USA